



HAL
open science

Fragmentation of magnetic particle aggregates in turbulence

H.M. de La Rosa Zambrano, G. Verhille, P. Le Gal

► **To cite this version:**

H.M. de La Rosa Zambrano, G. Verhille, P. Le Gal. Fragmentation of magnetic particle aggregates in turbulence. 2018. hal-01784756

HAL Id: hal-01784756

<https://hal.science/hal-01784756>

Preprint submitted on 3 May 2018

HAL is a multi-disciplinary open access archive for the deposit and dissemination of scientific research documents, whether they are published or not. The documents may come from teaching and research institutions in France or abroad, or from public or private research centers.

L'archive ouverte pluridisciplinaire **HAL**, est destinée au dépôt et à la diffusion de documents scientifiques de niveau recherche, publiés ou non, émanant des établissements d'enseignement et de recherche français ou étrangers, des laboratoires publics ou privés.

Version 9 as of April 17, 2018
To be submitted to PRF.

Fragmentation of magnetic particle aggregates in turbulence

H.M. De La Rosa Zambrano, G. Verhille and P. Le Gal

Aix Marseille Univ, CNRS, Centrale Marseille, IRPHE, Marseille, France

(Dated: April 17, 2018)

Particle aggregation is an ubiquitous phenomenon encountered in many natural and industrial environments. We describe here the equilibrium state of the aggregation/fragmentation process of inertial **scale** particles clustering in turbulence *i.e.* when the particles and the aggregates are larger than the Kolmogorov dissipative scale η . For this purpose, we seeded a high Reynolds number turbulent von Kármán flow with millimetric nearly neutrally buoyant magnetic particles. Each magnetic dipole imposes a torque and a force on the other magnets at the origin of the cohesion of the aggregates. On the contrary, turbulent fluctuations impose external stresses which tend to fragment the aggregates. Using video image analyses, we have performed the three-dimensional reconstruction of the aggregates and measured their characteristic sizes. The average number of particles inside each aggregate as a function of the intensity of turbulence can then be deduced. Assuming a Kolmogorov inertial scaling law for the turbulent velocity increments, we predict theoretically the aggregate mean size which is in agreement with our experimental results.

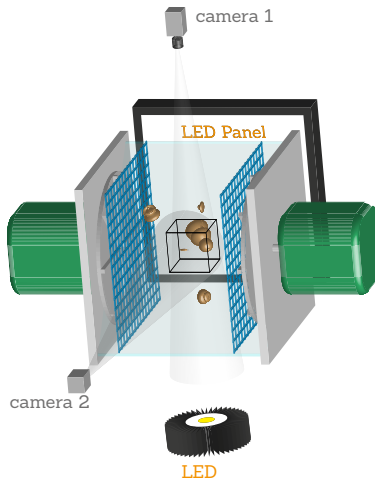


FIG. 1. Sketch of the turbulent von Kármán flow setup.

I. INTRODUCTION

The study of aggregation and fragmentation of flocs in turbulent flows is of great importance in engineering processes such as in the paper or textile making industry [1] where aggregation of particles or fibers is harmfully controlled. Aggregation is also very frequently observed in natural systems where it concerns a huge range of scales from nano or micro organic particles that can be transported by winds or marine currents [2] to dust grains and even rocks that aggregate in accretion disks during planet formation [3]. If the effects of turbulence on aggregation and fragmentation have been widely studied for particles whose size is within the viscous range of turbulence [4, 5], its consequences within the inertial range are poorly documented and not yet understood [6] despite their tremendous importance.

In the present study, we analyse the effect of a turbulent flow acting on aggregates of magnetic beads whose sizes are within the inertial range of turbulence. We performed a three-dimensional video image analysis to detect the aggregates and measure their characteristic sizes. While low intensity turbulence allows large aggregates, strong turbulence favors small aggregates: an equilibrium average size being reached when fragmentation by turbulence is balanced by the aggregation of individual particles on existing clusters or by the merging of smaller clusters [7]. Using Kolmogorov scaling arguments we propose a theoretical model whose predictions are validated by our experiments that are performed in a fully turbulent von Kármán flow. We choose millimetric magnetic particles because the separation force between two adjacent magnets is well characterized and relatively uniform through the thousand of particles we use. Then we will use a fractal description of the aggregate shapes to measure their dimensions in order to predict their average size as a function of the turbulence intensity.

II. EXPERIMENTAL SET-UP AND MEASUREMENT TECHNIQUES.

The turbulence is generated in the so called von Kármán flow by the counter-rotation of two impellers of radius $R = 8.6$ cm, fitted with straight blades ($h = 5$ mm), that can rotate at a controlled frequency f ranging from 8.5 to 30 Hz. FIG. 1 shows a drawing of our set-up that differs from classical installations [8, 9] by the presence of two grids parallel

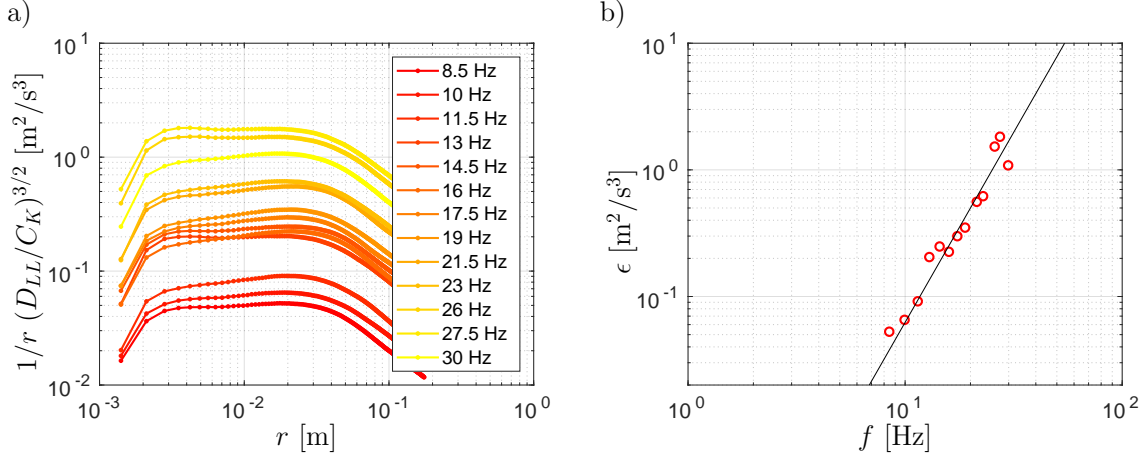


FIG. 2. a) Normalized longitudinal second-order velocity structure function for the different impeller rotation frequencies f . b) Energy dissipation rate ϵ as a function of the impellers rotation frequency f .

to the disks. The purpose of these grids is to avoid the aggregates to get close to and break on the rotating disks. The transparent acrylic cubic container is filled with 8 liters of water and the visualization is performed through two of its perpendicular sides. **With the help of LED light sources, diffused by a translucent screen, an homogeneous backlight is obtained and used to image the aggregates allowing good contrast and depth of the visual field.**

In order to characterize the turbulence, we have measured its properties by Particle Image Velocimetry (PIV) [10] in a 11 cm x 17 cm section of a meridional plane between the grids. Let us note that the turbulent kinetic energy $\langle u^2 \rangle$ is at least 5 times the mean flow energy $\langle u \rangle^2$. From the 2D PIV velocity fields, we can also measure the energy dissipation rate which is estimated using the longitudinal second-order velocity structure function $D_{LL}(r) \equiv \langle (u(x+r, t) - u(x, t))^2 \rangle$ where r is the spatial variable [11–13]. FIG. 2a) shows the variation of $D_{LL}(r)^{3/2}/r$ (normalized by the Kolmogorov constant C_K) as a function of r for different disk frequencies. In each case, the inertial regime corresponds to the plateaus extending between ~ 1 mm (larger than η because of the limited resolution of the PIV measure) and the integral scale $L_i \sim 3$ cm. **The typical length of an aggregate L_{ag} is smaller than the integral scale ($L_{ag} \sim 1$ cm). At this scale the pressure force induced by the mean flow is much smaller than the one due to turbulence. Hence, the aggregate will be mainly sensitive to the turbulent fluctuations.** The energy dissipation rate ϵ is given by the amplitude of these plateaus using a Kolmogorov constant $C_K = 2.12$ [14]. The variation of ϵ with the rotation frequency f is plotted in FIG. 2b). As expected, ϵ varies with the third power of f : $\epsilon = (2\pi\alpha)^3 R^2 f^3$, in agreement with classical results in turbulent von Kármán flow [8, 15], where here $\alpha = 3.24 \times 10^{-2}$. TABLE I summarizes the turbulence parameters.

The one thousand beads used for the experiments were made from 1 mm in diameter spherical neodymium magnets. In order to characterize the magnetic interaction, the separation force of a sample of magnetic bead pairs is measured when the pairs are separated by a stepper motor. At contact, the separation force is equal to 0.135 N. FIG. 3a) shows the evolution of the attractive force between two magnets with parallel magnetic momentum \mathbf{m} . As expected, this force decreases as r_b^{-4} , where r_b is the distance between the two dipoles [16]. Let us remark two important features that prevent the direct use of these magnetic beads:

Energy dissipation, ϵ	$0.05 - 2 \text{ m}^2/\text{s}^3$
Taylor microscale, $\lambda = \sqrt{15\nu u_{rms}^2/\epsilon}$	$1.6 - 3.2 \text{ mm}$
Taylor-Reynolds number, $Re_\lambda = \sqrt{15/\nu\epsilon} u_{rms}^2$	$600 - 1000$
Kolmogorov length scale, $\eta = (\nu^3/\epsilon)^{1/4}$	$28 - 65 \text{ }\mu\text{m}$
Integral scale, L_i	3 cm

TABLE I. Principal characteristics of turbulence.

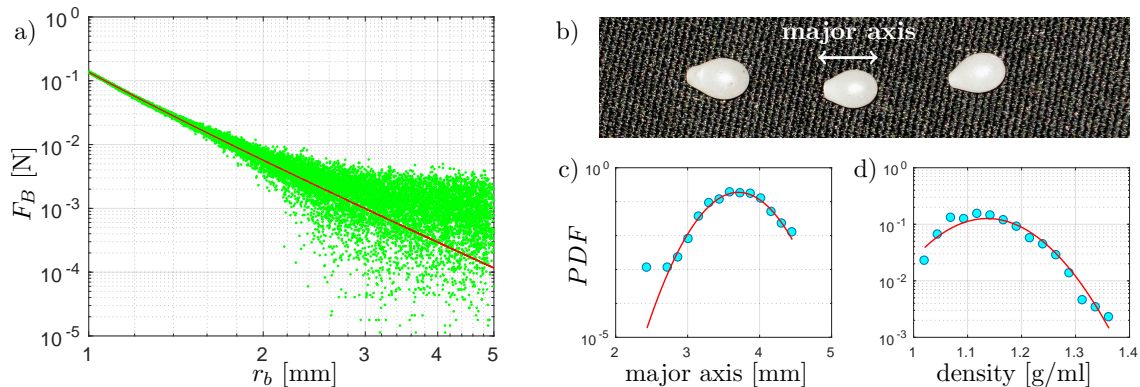


FIG. 3. a) Magnetic force F_B between the magnets as a function of their separation distance r . b) Photograph of some beads coated by wax. c) Main axis length probability distribution function (PDF) and d) density PDF, with their Gaussian fit.

first, their density being around 7, they would sink in water to the bottom of the container, and second, the separation force at contact would be too large compared to the expected hydrodynamic force thus preventing any fragmentation of the clusters by turbulence. Because of these two difficulties, we coated the magnets with a layer of wax which has two benefic effects: first, it reduces the apparent density of the particles and second, by increasing the bead diameter, it decreases the cohesion force at the contact. The characteristic of the final wax coated beads are presented in FIG. 3b), c) and d), where it can be seen that their shape is ovoidal because of the manufacturing process dipping them into melted wax. They have an aspect ratio around 1.5, an average main axis equal to 3.7 mm, a mean density of 1.14. Furthermore, the attractive force F_B is decreased and equal to $4 \cdot 10^{-4}$ N for a separation distance of 3.7 mm corresponding to the average major axis along which the magnetic dipole is aligned. To test the eventual role of the bouyancy during the aggregation/fragmentation process, some of our experimental runs were performed with salty water having a density of 1.14. As we will see later, very limited effects of sedimentation were detected, and most of our experimental runs were finally realized with fresh water.

IV. EXPERIMENTAL PROCEDURES AND MEASUREMENTS.

In order to relate the size of the aggregates to the intensity of turbulence, different experimental runs were performed at different rotation frequencies. At the beginning of each experiment, all the magnetic beads are placed inside the tank packed in a single large

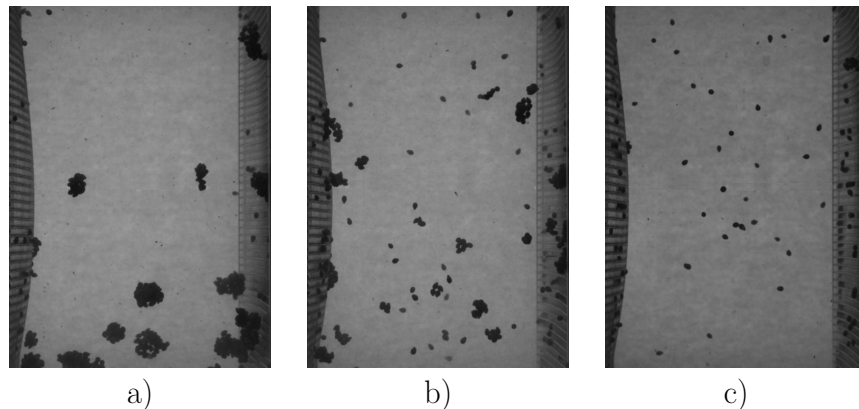


FIG. 4. Observation of the three different regimes as a function of the turbulence intensity. a) $f = 8.5$ Hz, b) $f = 14.5$ Hz, c) $f = 19$ Hz.

cluster, then the disks are set into rotation. Under the action of turbulence, the initial large aggregate breaks into smaller ones of different sizes. After some time, an equilibrium state is reached where the accretion of single particles or of small clusters versus the fragmentation of aggregates equilibrates. For each frequency, when the stationary regime is achieved (and checked by visual inspection), we record with two synchronized CCD cameras, a 255 or 500 frame video sequence of the flow at a rate of 5 images per second. We choose on purpose a low video rate in order to perform statistics of the aggregate size from uncorrelated images. Three different regimes are detected and illustrated in FIG. 4. As expected, at a low frequency (8.5 Hz on FIG. 4a) the aggregates are made of a relatively large number of magnets; while at higher frequency, the size of the aggregates becomes smaller (see FIG. 4b) for 14.5 Hz) until the flow is seeded by merely only individual particles (see FIG. 4c) for 19 Hz).

To measure the average volumes of the aggregates, we have performed a three-dimensional digital reconstruction of each of them using the convex hull volume reconstruction method [17]. As shown in [18], the precision of the volume reconstruction increases with the number of cameras. Here with only two cameras, the volumes are always overestimated by this measurement. However, most of the time the shape of the aggregates is not concave, then this error should not impact our results. Moreover, the packing coefficients, introduced later in the next section, will consider the concavity of the aggregates. The principle of the reconstruction is the following: an initial cubic volume is determined at the center of the tank, a region seen by both cameras. This volume is then divided in 8 cubes with equal side which are projected on the two images. If the projection of a cube is empty in at least one image, this cube is discarded. Otherwise, this cube is divided into 8 smaller cubes and the process is repeated until the current cube is completely filled and then saved. Finally, the volume of each aggregate is determined using the positions and the sizes of each saved cube.

V. A MODEL FOR THE AGGREGATE EQUILIBRIUM SIZE.

On average, aggregates are constituted by a number N of magnetic particles of diameter d . We can then express their average volume V , cross section area S and length L as a function of N and d :

$$V = c_3 N^{3/d_3} d^3, \quad S = c_2 N^{2/d_2} d^2, \quad L = c_1 N^{1/d_1} d \quad (1)$$

where $1/d_1$, $2/d_2$ and $3/d_3$ are fractal dimensions characterizing the shapes of the aggregates and c_1 , c_2 and c_3 three parameters representing their level of packing. From the inspection of the aggregates as can be seen on FIG. 4, they appear to be quite compact without any arborescence. As a consequence and in order to simplify our analysis we will assume in the following that $d_3 = 3$, and thus will keep the possible fractal arrangements of clusters only in the expressions of S and L . **Following the seminal idea of Kolmogorov [19]** concerning drop breakage in turbulence, we show now that the mean size of the aggregates is given by the balance between the hydrodynamic force F_H acting on their cross section and the magnetic force F_B that tends to keep two particles clustered together. Indeed, when an aggregate breaks into smaller ones, the last link between the initial aggregate and a particle (belonging or not to another cluster) is controlled by a unique dipolar interaction *i.e.* by the force F_B . This assumption differs strongly from the classical hypothesis where the number of broken bonds scales with the number of aggregated particles [20]. Here the aggregates have a mean size L within the inertial range of turbulence. Then the hydrodynamic force F_H applied on the aggregate is driven by the pressure [21]:

$$F_H = \frac{1}{2}\rho(\delta u_L)^2 S \quad (2)$$

where δu_L is the typical velocity increment at scale L and ρ the fluid density. Taking into account that $\delta u_L = (\epsilon L)^{1/3}$, that is the classical law of homogeneous and isotropic turbulence [12] together with our measurement of the dissipation rate ϵ , we can express the equilibrium regime of the fragmentation/aggregation process:

$$F_H = 2\rho(\alpha\pi f)^2 (R^2 d^4 N^\beta)^{2/3} c_2 c_1^{2/3} = F_B \quad (3)$$

with $\beta = (3d_1 + d_2)/d_1 d_2$. For high rotation rates of the impellers, we have observed that aggregates are completely fragmented and that only individual particles are present in the flow (see FIG. 4c). Therefore aggregates reach their smallest size when they are constituted by only $N_c = 2$ beads *i.e.* chain-like structures implying that $c_1 = 1$, $c_2 = \pi/4$, $c_3 = \pi/6$, $d_1 = 1$ and $d_2 = 2$ giving $\beta_c = 5/2$. A threshold frequency f_c for the aggregation onset is thus obtained from equation (3). For our set-up, we calculate a value $f_c \approx 25$ Hz. This value corresponds to a dissipation rate $\epsilon_c \sim 1$ m²/s³. Using this threshold, we can recast equation (3) to predict the average number of particles per aggregate:

$$N = \left(\frac{f_c}{f}\right)^{3/\beta} \left(\frac{N_c}{a}\right)^{\beta_c/\beta} \quad \text{or} \quad N = \left(\frac{\epsilon_c}{\epsilon}\right)^{1/\beta} \left(\frac{N_c}{a}\right)^{\beta_c/\beta} \quad (4)$$

with $a = (4/\pi c_1^{2/3} c_2)^{3/2\beta_c}$. As $\beta_c = 5/2$, $a = (4/\pi c_1^{2/3} c_2)^{3/5}$, a value that remains close to 1 for the different arrangements that can be encountered for packing beads [22].

As can be observed on FIG. 4a), in the low frequency or weakest turbulence regime, the aggregates seem quite smooth and compact. In this case $d_1 = d_2 = 3$ and $\beta = 4/3$. As a consequence, equation (4) leads to a scaling law valid far from the aggregation onset for the average number N of particles per aggregate as a function of the rotation frequency f of the disks or of the dissipation rate of turbulence:

$$N \propto \left(\frac{f}{f_c}\right)^{-9/4} \quad \text{or} \quad N \propto \left(\frac{\epsilon}{\epsilon_c}\right)^{-3/4} \quad (5)$$

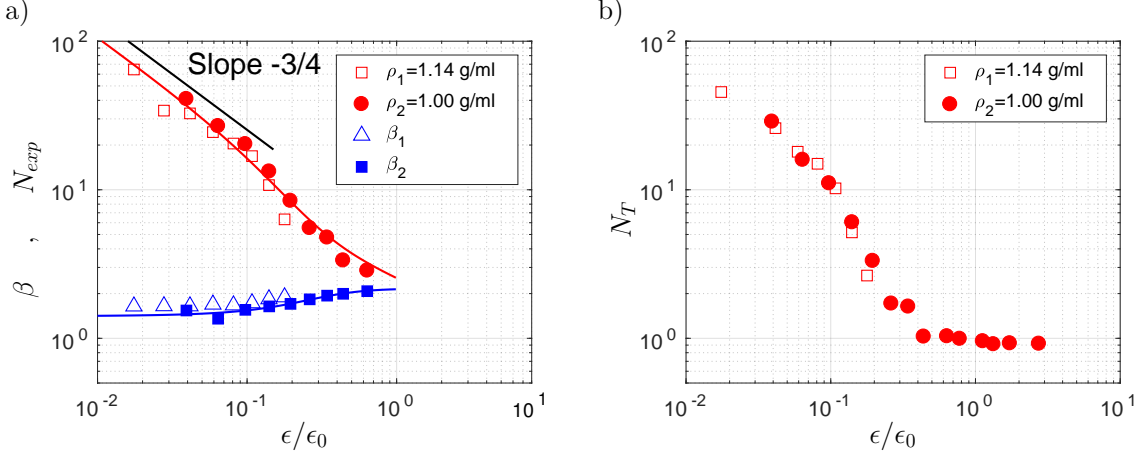


FIG. 5. a) Experimental results for fresh water: red filled circles (N_{exp}) and blue filled squares (β) and salt water results: red empty squares (N_{exp}) and blue empty triangles (β) and theoretical predictions (solid lines) of the average number of particles N per aggregate, versus the dissipation rate ϵ of turbulence. A smooth sigmoid evolution for β is fitted through the fresh water data and is used together with the measured threshold $f_c = 25$ and fitting parameter $a = 0.9$ and $6c_3/\pi = 1$ to predict N_{exp} . b) Measure of the average number N_T of particles per aggregate taking into account individual particles in the statistics.

A similar scaling law is predicted in [20] but the assumption on the number of bonds broken at fragmentation leads to a different exponent. **These results are analogous to the pioneer work of Kolmogorov on the drop fragmentation in turbulence where the size of the droplet D_{drop} is related to the turbulent intensity: $D_{drop} \sim \epsilon^{-K}$ with $K = 2/5$ [19].**

VI. COMPARISON BETWEEN EXPERIMENTAL RESULTS AND THEORY.

After having processed the synchronized video images issued from the two cameras, a statistical study of the aggregate size and shape distribution is realized. Note that as our model applies only for $N \geq 2$, the individual particles are not taken into account in the statistical analysis. First, the measurement for each aggregate of its surface S and length L versus its volume V leads to the determination of the average d_1 and d_2 and β which is plotted on FIG. 5a) versus ϵ/ϵ_c together with its fit. FIG. 5a) presents also the evolution of the measured average number N_{exp} of particles per aggregate for the two different densities of fresh and salty water. N_{exp} is calculated from the volume of each aggregate divided by the volume $\pi d^3/6$ of a single particle. It is then an upper bound of the real number of particles N that depends on the packing number c_3 : $N_{exp} = 6c_3/\pi N$ with c_3 between $\pi/6$ for chains and $1/\sqrt{2}$ for the maximum admissible packing of spheres [22]. **We can conclude that the value of c_3 is quite constraint and stays in any case close to 0.5 thus justifying our choice to keep $c_3 = \pi/6$.** Using a smooth sigmoid function $\beta_{fit} = \beta_0/(1 + \exp((\epsilon - \epsilon_b)/\sigma)) + \beta_\infty$ that fits the experimental values of β together with the threshold value found theoretically and a fitting coefficient $a = 0.9$ and $6c_3/\pi = 1$, we see that our theoretical model nicely reproduces the experimental results on the entire range of exploration (solid lines on FIG. 5a)). Between the large and smooth aggregate asymptotic regime given by the $-3/4$ scaling law (5) and the aggregation threshold, there exists a smooth transition where the shape of the aggregates

becomes less regular, acquiring non trivial fractal dimensions. Finally, under the threshold, the average measured number N_T of aggregated *or not* particles, becomes close to the single particle limit as can be observed in FIG. 5b). We also observe that the results of the experiments using fresh and salty water are very close one to the other, justifying our assumption to neglect the settling.

VII. CONCLUSIONS.

In classical studies on aggregation of nano or micro particles in turbulent flows, those are usually smaller than the Kolmogorov's scale of turbulence and thus are essentially sensitive to viscous effects. In this study, we have deliberately chosen to study the fragmentation of particle aggregates whose sizes are within the inertial range of turbulence. Experiments were performed using in house manufactured millimetric magnetic particles that aggregate thanks to their magnetic field. The consideration of a classical model of turbulence based on Kolmogorov similarity hypothesis leads to the prediction of the average size of the aggregates as a function of the turbulence intensity. Experimental measurements - using an original three dimensional aggregate detection and reconstruction software - and theoretical predictions agree very well. Therefore, we claim that knowing the intensity of turbulence, and knowing the cohesive force and shapes of the particles, our model can predict the average size of the aggregates. We expect that our result can be used in different engineering situations but we claim also that it can be used to probe turbulence itself: knowing the force field between particles, the sole observation of the aggregate sizes and shapes should lead to the estimation of the level of turbulence.

This work has been carried out in the framework of the Labex MEC Project (No. ANR-10-LABX-0092) and of the A*MIDEX Project (No. ANR-11-IDEX-0001-02), funded by the 'Investissements d'Avenir' French Government program managed by the French National Research Agency (ANR). HDLR would like to thank CONACYT for his international PhD grant.

-
- [1] Fredrik Lundell, L. Daniel Söderberg, and P. Henrik Alfredsson. Fluid Mechanics of Papermaking. *Annual Review of Fluid Mechanics*, 43(1):195–217, 2011.
 - [2] Charles B. Miller. *Biological Oceanography*. John Wiley & Sons, April 2009.
 - [3] Jürgen Blum and Gerhard Wurm. The Growth Mechanisms of Macroscopic Bodies in Protoplanetary Disks. *Annual Review of Astronomy and Astrophysics*, 46(1):21–56, 2008.
 - [4] Matthäus U. Bäbler, Massimo Morbidelli, and Jerzy Baldyga. Modelling the breakup of solid aggregates in turbulent flows. *Journal of Fluid Mechanics*, 612:261–289, October 2008.
 - [5] Alain Pumir and Michael Wilkinson. Collisional Aggregation Due to Turbulence. *Annual Review of Condensed Matter Physics*, 7(1):141–170, 2016.
 - [6] Benjamin Oyegbile, Peter Ay, and Satyanarayana Narra. Flocculation kinetics and hydrodynamic interactions in natural and engineered flow systems: A review. *Environmental Engineering Research*, 21(1):1–14, March 2016.
 - [7] M von Smoluchowski. Drei Vortrage uber Diffusion. Brownsche Bewegung und Koagulation von Kolloidteilchen. *Z. Phys*, 17:557–585, 1916.

- [8] Florent Ravelet. *Bifurcations globales hydrodynamiques et magnétohydrodynamiques dans un écoulement de von Karman turbulent*. phdthesis, Ecole Polytechnique X, September 2005.
- [9] Nathanaël Machicoane, Robert Zimmermann, Lionel Fiabane, Mickaël Bourgoïn, Jean-François Pinton, and Romain Volk. Large sphere motion in a nonhomogeneous turbulent flow. *New Journal of Physics*, 16(1):013053, 2014.
- [10] William Thielicke and Eize Stamhuis. PIVlab – Towards User-friendly, Affordable and Accurate Digital Particle Image Velocimetry in MATLAB. *Journal of Open Research Software*, 2(1), October 2014.
- [11] Stephen B. Pope. Turbulent Flows. *Measurement Science and Technology*, 12(11):2020, 2001.
- [12] AN Kolmogorov. Dissipation of energy in locally isotropic turbulence [In Russian]. *Dokl. Akad. Nauk SSSR*, 32:19–21, 1941.
- [13] Duo Xu and Jun Chen. Accurate estimate of turbulent dissipation rate using PIV data. *Experimental Thermal and Fluid Science*, 44(Supplement C):662–672, January 2013.
- [14] Katepalli R. Sreenivasan. On the universality of the Kolmogorov constant. *Physics of Fluids*, 7(11):2778–2784, November 1995.
- [15] R. Labbé, J.-F. Pinton, and S. Fauve. Power Fluctuations in Turbulent Swirling Flows. *Journal de Physique II*, 6(7):1099–1110, July 1996.
- [16] L. D. Landau, J. S. Bell, M. J. Kearsley, L. P. Pitaevskii, E. M. Lifshitz, and J. B. Sykes. *Electrodynamics of Continuous Media*. Elsevier, October 2013.
- [17] Kong-man (German) Cheung, Simon Baker, and Takeo Kanade. Shape-From-Silhouette Across Time Part I: Theory and Algorithms. *International Journal of Computer Vision*, 62(3):221–247, May 2005.
- [18] D. Adhikari and E. K. Longmire. Visual hull method for tomographic PIV measurement of flow around moving objects. *Experiments in Fluids*, 53(4):943–964, October 2012.
- [19] A. KOLMOGOROV. On the breakage of drops in a turbulent flow. *Dokl. Akad. Nauk. SSSR*, 66:825–828, 1949.
- [20] D. H. Bache. Floc rupture and turbulence: a framework for analysis. *Chemical Engineering Science*, 59(12):2521–2534, June 2004.
- [21] Nauman M. Qureshi, Mickaël Bourgoïn, Christophe Baudet, Alain Cartellier, and Yves Gagne. Turbulent Transport of Material Particles: An Experimental Study of Finite Size Effects. *Physical Review Letters*, 99(18):184502, October 2007.
- [22] J. H. Conway and N. J. A. Sloane. *Sphere Packings, Lattices, and Groups*. Springer, New York, 2 edition, 1993.